High Efficient and Robust Quantum Watermarking Algorithm Based on Quantum Log-polar Images and Matrix Coding

Zhiguo Qu[1], Zhenwen Cheng[2], Mingming Wang[3], Wenjie Liu[1]

[1] Jiangsu Engineering Center of Network Monitoring, Nanjing University of Information Science and Technology, China
[2] School of Electronic & Information Engineering, Nanjing University of Information Science and Technology, China
[3] School of Computer Science, Xi'an Polytechnic University, China
qzghhh@126.com, czw381576996@163.com, bluess1982@126.com, wenjiel@163.com

Abstract

With the development of quantum computer and quantum network, the security of quantum images has been becoming more and more important in the 21st century. In this paper, a high efficient and robust quantum watermarking algorithm is proposed to better protect copyright of quantum images, which is based on quantum log-polar image (QUALPI) representation model, matrix coding and the least significant qubit (LSQb) modification technique. By taking advantage of QUALPI representation model's two important properties, i.e., rotation and scale invariances, the new algorithm makes quantum watermark image extracted having a good robustness when stego image was subjected to geometric attacks, such as rotation and scaling. In addition, by adopting matrix coding and the LSQb modification technique, the new algorithm can achieve great transparency for high embedding efficiency and low modification rate. Experimental simulation based on MATLAB shows that the new algorithm has a good performance on robustness and transparency as the conclusions.

Keywords: Quantum watermarking algorithm, Quantum log-polar image, Matrix coding, Least significant qubit, Robustness

1 Introduction

As a new discipline, quantum information technology effectively combines the characteristic of quantum mechanics and information science. Copyright protection of quantum images is one of the research fields in quantum information hiding, which is an important branch of information security [1-2] in quantum networks. In order to transmit multimedia information securely in quantum networks, quantum images denoted by quantum states have been widely used to store and transfer digital image information in recent decades. As a result, quantum watermarking, that embeds quantum watermark image consisting of information about copyright owner into quantum carrier image, has emerged to protect copyright of quantum images.

So far, many quantum image representation models, i.e., Qubit Lattice [3], Entangled Image [4], Real Ket [5], flexible representation of quantum images (FRQI) [6], novel enhanced quantum representation (NEQR) [7], quantum log-polar image (QUALPI) [8] and novel quantum representation of color digital images (NCQI) [9] have been proposed to utilize quantum states to store image information. Among of them, more geometric transformations on quantum images can be performed easily based on QUALPI, including those complex ones such as rotation and scale. In term of performance improvement in digital image processing, the utilization of quantum image analysis, for example quaternion Zernike moments (QZMs) [10], content-based image retrieval (CBIR) [11] and digital image forensics [12], also has been quite successful.

Generally speaking, quantum watermarking is the technique which embeds the invisible quantum information (such as the owner's identification or ownership certificate) into quantum multimedia data (such as quantum audio, video or image) as carrier for copyright protection. There are mainly three key performance parameters for quantum watermarking, i.e., robustness, transparency and capacity, according to their respective importance in turn. For many quantum watermarking algorithms, how to balance robustness and transparency is a main issue that is needed to be carefully solved.

For quantum audio watermarking, Zhang Yipeng et al. proposed two quantum audio watermarking algorithms using quantum neural networks [13] and improved quantum neural networks [14], respectively. As for quantum video watermarking, there is hardly ever put forward except that Gao Qi et al. proposed a blind quantum video watermarking algorithm based on correlations between neighboring frames [15] in 2006, and Iliyasu proposed video processing applications on quantum computers [16] in 2013. In aspect of quantum

*Corresponding Author: Zhiguo Qu; E-mail: qzghhh@126.com
DOI: 10.3966/160792642018111906019

image watermarking, the least significant qubit (LSQb) modification technique is one of the most widely used methods, which has advantages of easy operation and large payload. In 2016, a LSQb modification algorithm for quantum image based on NCQI representation model [17] was proposed by Sang et al. Thereafter, more quantum image watermarking algorithms were proposed by adopting various methods. For example, Song Xianhua et al. and Yang Yuguang et al. proposed quantum watermarking algorithms for quantum images based on Hadamard transform [18] and quantum Fourier transform [19], respectively. These two algorithms have a larger capacity and good transparency.

In general, based on the existing achievements mentioned above, it's easy to know that quantum watermarking is still on the early stage of its development currently. Most of quantum image watermarking algorithms have not yet begun to discuss the robustness of watermark image, especially on geometric attacks. In view of widespread applications and universality of geometric attacks in quantum image processing, many watermarked quantum images are invulnerable to resist this kind of attacks. Furthermore, due to the conflicting balance between robustness and transparency, many quantum image watermarking algorithms are with weak robustness or poor transparency. In order to simultaneously improve robustness and transparency, the watermarking algorithms [20-22] were proposed to achieve this goal by sacrificing a relatively less important performance, capacity of watermark. Following this idea and also in order to make up for the robustness drawbacks of existing quantum image watermarking algorithms, this paper proposes a high efficient and robust quantum watermarking algorithm based on QUALPI representation model and matrix coding [23]. By combining QUALPI representation model with matrix coding and the LSQb modification technique, the new algorithm enables to effectively resist geometric distortions or attacks and further improve transparency of watermark image for high embedding efficiency and low modification rate, so as to better protect copyright of quantum images.

The rest of the paper is organized as follows. Section 2 introduces the preliminary knowledge related to the new algorithm. In Section 3, the new quantum watermarking algorithm is described in detail. The simulation results and performance analysis are given in Section 4. Finally, a conclusion and the future work are provided in Section 5.

2 Preliminaries

2.1 Quantum Representation for Log-polar Images

In quantum log-polar image (QUALPI) representation model, the size range of the log-radius ρ, the angular θ and the gray scale $g(\rho,\theta)$ are assumed to be 2^m, 2^n and 2^q, respectively. And $g(\rho,\theta)$ can be encoded by the binary sequence $C_{q-1}C_{q-2}\cdots C_1C_0$ as follow.

$$g(\rho,\theta)=C_{q-1}C_{q-2}\cdots C_1C_0, C_i\in\{0,1\}, g(\rho,\theta)\in\left[0,2^{q-1}\right] \quad \textbf{(1)}$$

For this image, the representation can be expressed in term of Equation (2). Equation (2) indicates that the whole QUALPI is stored in a normalized and equiprobable quantum superposition, in which each basis state represents one pixel.

$$|I\rangle=\frac{1}{\sqrt{2^{m+n}}}\sum_{\rho=0}^{2^m-1}\sum_{\theta=0}^{2^n-1}\left(|g(\rho,\theta)\rangle\otimes|\rho\rangle\otimes|\theta\rangle\right) \quad \textbf{(2)}$$

Figure 1 demonstrates an example of a $2^1\times 2^2$ log-polar image with gray range 256, i.e., m=1, n=2 and q=8. It is obvious that all pixels are stored in a normalized quantum superposition $|I\rangle$.

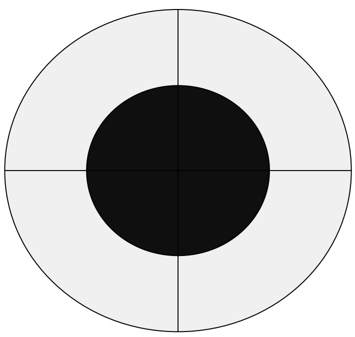

$$|I\rangle=\frac{1}{2\sqrt{2}}\Big[|00001111\rangle\otimes\left(|000\rangle+|001\rangle+|010\rangle+|011\rangle\right)+ |11110000\rangle\otimes\left(|100\rangle+|101\rangle+|110\rangle+|111\rangle\right)\Big]$$

Figue 1. A $2^1\times 2^2$ quantum log-polar image and its quantum expression of QUALPI

2.2 Quantum Rotation Transformation of QUALPI

Firstly, quantum unit rotation transformation based on QUALPI representation model is discussed in Ref [8]. For this transformation, all pixels of QUALPI will rotate counter-clockwise by one unit. And it will add the angular positions of every pixel by 1 (mod 2^n). The quantum unit rotation operation is defined as R_1 in term of Equation (3).

$$R_1|I\rangle = R_1\left(\frac{1}{\sqrt{2^{m+n}}}\sum_{\rho=0}^{2^m-1}\sum_{\theta=0}^{2^n-1}|g(\rho,\theta)\rangle\otimes|\rho\rangle\otimes|\theta\rangle\right) = \frac{1}{\sqrt{2^{m+n}}}\sum_{\rho=0}^{2^m-1}\sum_{\theta=0}^{2^n-1}\left(|g(\rho,\theta)\rangle\otimes|\rho\rangle\otimes|(\theta+1)\bmod 2^n\rangle\right) \quad \textbf{(3)}$$

Next, quantum arbitrary rotation transformation of QUALPI is discussed by utilizing some unit rotations to accomplish it. Assuming that the rotation angle A_x can be encoded as follow.

$$A_x = r_{n-1}r_{n-2}\cdots r_1 r_0, r_k \in \{0,1\}, A_x \in \left[0, 2^n - 1\right] \quad \textbf{(4)}$$

When an arbitrary rotation transformation R_x is operated on QUALPI, the procedure can be divided into n sub-operations. If r_k=0, the k_{th} sub-operation will do nothing. Otherwise, it will make QUALPI to rotate counter-clockwise at angle 2^k. And this operation R_{2^k} means to make a unit shift for the highest $(n-k)$ qubits of the angular sequence $|\theta\rangle$ in QUALPI. The quantum rotation operation R_{2^k} is defined in term of Equation (5).

$$\begin{aligned} R_{2^k}(|I\rangle) &= R_{2^k}\left(\frac{1}{\sqrt{2^{m+n}}}\sum_{\rho=0}^{2^m-1}\sum_{\theta=0}^{2^n-1}|g(\rho,\theta)\rangle\otimes|\rho\rangle\otimes|\theta\rangle\right) \\ &= \frac{1}{\sqrt{2^{m+n}}}\sum_{\rho=0}^{2^m-1}\sum_{\theta=0}^{2^n-1}\left(|g(\rho,\theta)\rangle\otimes|\rho\rangle\otimes|(\theta+2^k)\bmod 2^n\rangle\right) \\ &= \frac{1}{\sqrt{2^{m+n}}}\sum_{\rho=0}^{2^m-1}\sum_{\theta=0}^{2^n-1}\left(|g(\rho,\theta)\rangle\otimes|\rho\rangle \otimes|(\theta_{n-1}\theta_{n-2}\cdots\theta_k+1)\bmod 2^{n-k}\rangle\otimes|\theta_{k-1}\theta_{k-2}\cdots\theta_0\rangle\right) \end{aligned} \quad \textbf{(5)}$$

Finally, an arbitrary rotation can be decomposed into n rotation operations at most.

2.3 Matrix Coding

Matrix coding [23] is a widely used information coding. By adopting matrix coding, watermarking algorithm can own high embedding efficiency and low modification rate to obtain good transparency.

It's assumed that the least significant bit (LSB) of (2^k-1) carrier data, i.e., a_1, a_2, ..., and a_{2^k-1}, embed k secret bits, i.e., x_1, x_2, ..., and x_k. Before embedding secret bits into carrier data by matrix coding, the i_{th} carrier data' position is encoded as follow.

$$i = b_{i,k}b_{i,k-1}\cdots b_{i,1}, b_{i,j} \in \{0,1\}, j\in[1,k], i\in[1,2^k-1] \quad \textbf{(6)}$$

Then, c_j is calculated in term of Equation (7),

$$c_j = \begin{cases} 0, x_j = \overset{2^k-1}{\underset{i=1}{\oplus}}\left(a_i\cdot b_{i,j}\right) \\ 1, x_j \neq \overset{2^k-1}{\underset{i=1}{\oplus}}\left(a_i\cdot b_{i,j}\right) \end{cases} j\in[1,k] \quad \textbf{(7)}$$

where $\overset{2^k-1}{\underset{i=1}{\oplus}}$ denotes that a series of $a_i\cdot b_{i,j}$ are calculated by XOR operations.

Next, C can be represented in term of Equation (8). If C=0, there is nothing to do. Otherwise, a_C needs to be changed. At last, secret bits can be extracted according to Equation (9).

$$C = \sum_{j=1}^{k} c_j \cdot 2^{j-1} \quad \textbf{(8)}$$

$$x_j = \overset{2^k-1}{\underset{i=1}{\oplus}}\left(a_i\cdot b_{i,j}\right), j\in[1,k] \quad \textbf{(9)}$$

The utilization rate U of carrier data and the embedding rate E are defined as Equation (10) and (11), respectively.

$$U = \frac{k}{2^k-1} \quad \textbf{(10)}$$

$$E = \frac{2^k}{2^k-1}\cdot k \quad \textbf{(11)}$$

Table 1 shows the performances of matrix coding when k gets different values. When k=1, matrix coding is degenerated to the simple LSB modification technique. The larger k is, the lower the utilization rate but the higher the embedding efficiency will be.

Table 1. The performances of matrix coding when k gets different values

k	n	The utilization rate U of carrier data (%)	The embedding rate E
1	1	100.00	2.00
2	3	66.67	2.67
3	7	42.86	3.43
4	15	26.67	4.27
5	31	16.13	5.16
6	63	9.52	6.09
7	127	5.51	7.06
8	255	3.14	8.03
9	511	1.76	9.02

Taking k=2 for example, if

$$x_1 = a_1 \oplus a_3, x_2 = a_2 \oplus a_3 \quad \textbf{(12)}$$

it does not change carrier data. If

$$x_1 \neq a_1 \oplus a_3, x_2 = a_2 \oplus a_3 \quad \textbf{(13)}$$

it should change a_1. If

$$x_1 = a_1 \oplus a_3, x_2 \neq a_2 \oplus a_3 \quad \textbf{(14)}$$

it should change a_2. If

$$x_1 \neq a_1 \oplus a_3, x_2 \neq a_2 \oplus a_3 \quad \textbf{(15)}$$

it should change a_3. Equation (16) can be used to extract secret bits.

$$a_1' \oplus a_3' = x_1, a_2' \oplus a_3' = x_2 \quad \textbf{(16)}$$

2.4 Improved Quantum Comparator to Implement the LSQb Modification Technique

In order to realize the embedding process of quantum watermarking by using matrix coding and the LSQb modification technique, it is necessary that the LSQb of quantum carrier image is replaced by quantum watermark image. Inspired by Wang Dong's designed the quantum comparator [24] to judge whether two qubits are same or not, an improved quantum comparator also is designed in this paper, as shown in Figure 2.

In Figure 2, $|a\rangle$ and $|b\rangle$ are the input qubits, $|0\rangle$ is the auxiliary qubit, $|c\rangle$ and $|d\rangle$ are the output qubits. When $|a\rangle|b\rangle=|0\rangle|0\rangle$ or $|a\rangle|b\rangle=|1\rangle|0\rangle$, then $|c\rangle|d\rangle=|0\rangle|0\rangle$. When $|a\rangle|b\rangle=|0\rangle|1\rangle$ or $|a\rangle|b\rangle=|1\rangle|1\rangle$, then $|c\rangle|d\rangle=|1\rangle|1\rangle$. It can be known that $|a\rangle$ will be replaced by $|b\rangle$ by using the improved quantum comparator.

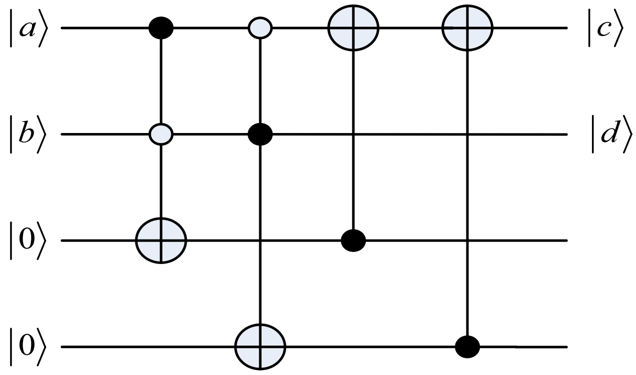

Figure 2. An improved quantum comparator

3 Efficient and Robust Quantum Watermarking Algorithm

In this section, the processes of embedding and extracting are presented in details. The whole process of the new algorithm is shown in Figure 3.

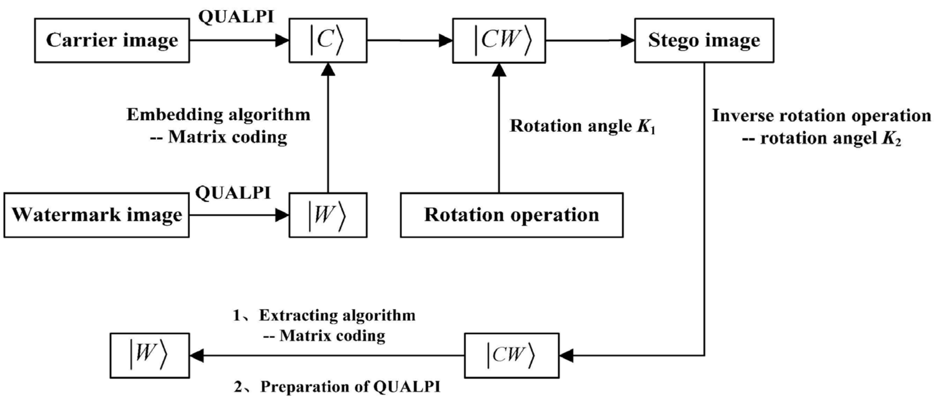

Figure 3. The flow chart of the new algorithm

3.1 The Embedding Process

According to QUALPI representation model and matrix coding introduced in Section 2, watermark image can be embedded into carrier image successfully. Its main steps are described as follows.

Step(1). At first, QUALPI quantum image is prepared from classical log-polar image. The QUALPI expressions of quantum carrier image (gray image) and quantum watermark image (binary image) are expressed as Equation (17) and (18), respectively.

$$|C\rangle=\frac{1}{\sqrt{2^{m+n}}}\sum_{\rho=0}^{2^m-1}\sum_{\theta=0}^{2^n-1}|c_7c_6\cdots c_0\rangle|\rho\theta\rangle \quad \textbf{(17)}$$

$$|W\rangle=\frac{1}{\sqrt{2^{e+f}}}\sum_{\rho=0}^{2^e-1}\sum_{\theta=0}^{2^f-1}|w\rangle|\rho\theta\rangle \quad \textbf{(18)}$$

Step(2). In order to apply the idea of matrix coding, the gray scale's LSQb $|c_0^{y,z}\rangle$, the (y, z) pixel of quantum carrier image, and $|w^{y,z}\rangle$ of quantum watermark image represent carrier data' LSQb and secret qubit mentioned in Section 2.3, respectively. The new algorithm adopts matrix coding with k=3 and n=7 to determine which LSQb values of quantum carrier image's pixels will be modified. In this case, Equation (9) is actually turned into Equations (19), (20) and (21) as follows.

$$|w^{3i-3}\rangle=|c_0^{7i-7}\rangle\oplus|c_0^{7i-5}\rangle\oplus|c_0^{7i-3}\rangle\oplus|c_0^{7i-1}\rangle \quad \textbf{(19)}$$

$$|w^{3i-2}\rangle=|c_0^{7i-6}\rangle\oplus|c_0^{7i-5}\rangle\oplus|c_0^{7i-2}\rangle\oplus|c_0^{7i-1}\rangle \quad \textbf{(20)}$$

$$|w^{3i-1}\rangle=|c_0^{7i-4}\rangle\oplus|c_0^{7i-3}\rangle\oplus|c_0^{7i-2}\rangle\oplus|c_0^{7i-1}\rangle \quad \textbf{(21)}$$

It's easy to know that no change will be made to quantum carrier image if $|w^{3i-3}\rangle$, $|w^{3i-2}\rangle$ and $|w^{3i-1}\rangle$ are satisfied with Equations (19), (20) and (21), where $1\le i\le 2^{e+f}/3$. Otherwise, according to Equations (7) and (8), one of seven LSQbs of quantum carrier image's pixels is needed to be modified for embedding quantum watermark image.

In addition, two parties of communication share the key (named as M) to determine where pixels of quantum carrier image will be used by matrix coding.

Step(3). In order to make the new algorithm having good practicability, a quantum circuit to implement the embedding process is designed, as shown in Figure 4. In Figure 4, $\left|c_0^S\right\rangle$ of quantum carrier image denotes the gray scale's LSQb in the S_{th} pixel to be modified for embedding, and $\left|w_0^S\right\rangle$ is the gray scale of quantum watermark image. The key M chooses one of these control boxes to determine which LSQbs will be modified in quantum carrier image. If so, the unitary operation $U_{D_{y,z}}$ will be performed on these LSQbs as follow.

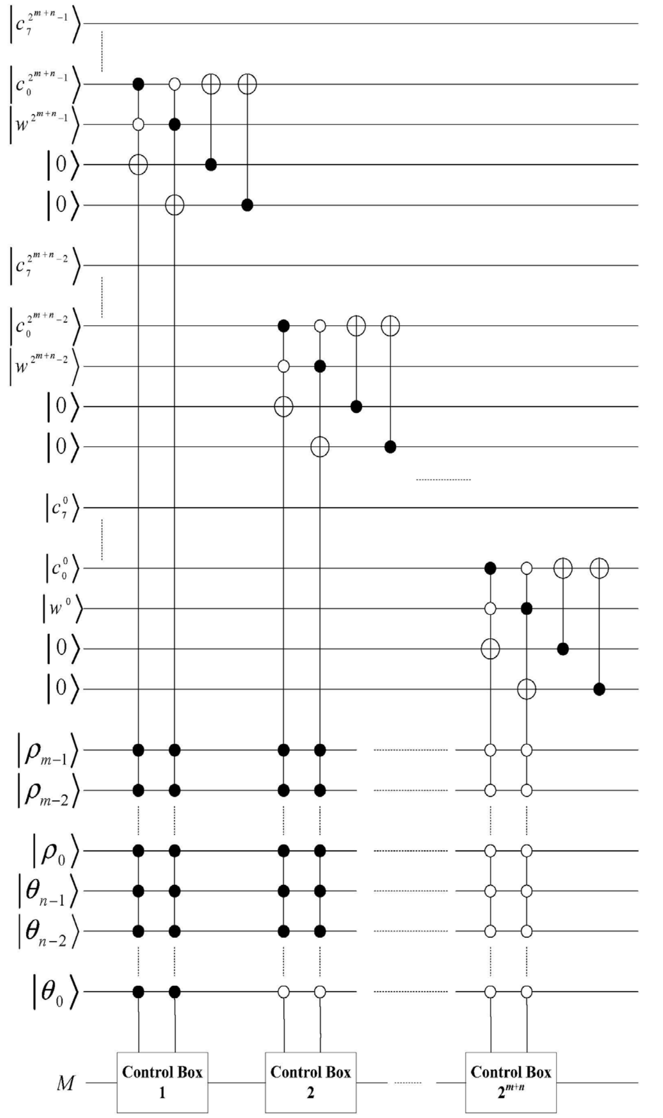

Figure 4. Quantum circuit implement of the embedding process

$$\begin{aligned}
U_{D_{yz}}(|C\rangle) &= \left(I^{\otimes q-1} \otimes U \otimes |yz\rangle\langle yz| + I^{\otimes q} \otimes \sum_{\rho=0}^{2^m-1} \sum_{\theta=0,\rho\theta\neq yz}^{2^n-1} |\rho\theta\rangle\langle\rho\theta| \right) \\
&\left(\frac{1}{\sqrt{2^{m+n}}} \sum_{\rho=0}^{2^m-1}\sum_{\theta=0}^{2^n-1} |c_{q-1}c_{q-2}\cdots c_1c_0\rangle|\rho\theta\rangle \right) \\
&= \frac{1}{\sqrt{2^{m+n}}} \left(I^{\otimes q-1} \otimes U \otimes |yz\rangle\langle yz| + I^{\otimes q} \otimes \sum_{\rho=0}^{2^m-1} \sum_{\theta=0,\rho\theta\neq yz}^{2^n-1} |\rho\theta\rangle\langle\rho\theta| \right) \\
&\left(|c_{q-1}^{yz}c_{q-2}^{yz}\cdots c_1^{yz}c_0^{yz}\rangle|yz\rangle + \sum_{\rho=0}^{2^m-1} \sum_{\theta=0,\rho\theta\neq yz}^{2^n-1} |c_{q-1}c_{q-2}\cdots c_1c_0\rangle|\rho\theta\rangle \right) \\
&= \frac{1}{\sqrt{2^{m+n}}} \left(|c_{q-1}^{yz}c_{q-2}^{yz}\cdots c_1^{ji}\overline{c_0}^{yz}\rangle|yz\rangle + \sum_{\rho=0}^{2^m-1} \sum_{\theta=0,\rho\theta\neq yz}^{2^n-1} |c_{q-1}c_{q-2}\cdots c_1c_0\rangle|\rho\theta\rangle \right)
\end{aligned} \tag{22}$$

Where

$$I = \sigma_I = \begin{bmatrix} 1 & 0 \\ 0 & 1 \end{bmatrix} \tag{23}$$

$$U = \sigma_X = \begin{bmatrix} 0 & 1 \\ 1 & 0 \end{bmatrix} \tag{24}$$

$$\left|\overline{c_0}^{yz}\right\rangle = \begin{cases} |0\rangle, \left|c_0^{yz}\right\rangle = 1 \\ |1\rangle, \left|c_0^{yz}\right\rangle = 0 \end{cases} \tag{25}$$

By repeating ***Step (2)***, quantum watermark image can be embedded into quantum carrier image to get stego image, which expression is given in term of Equation (26).

$$|C'\rangle = \frac{1}{\sqrt{2^{m+n}}} \sum_{\rho=0}^{2^m-1}\sum_{\theta=0}^{2^n-1} \left|c_7c_6\cdots c_0'\right\rangle|\rho\theta\rangle \tag{26}$$

Step(4). Finally, as described in Section 2.2, stego image will be made a rotation transformation R_x to prevent the third party from knowing the presence of quantum watermark image. The rotation angle K_1 can be determined by another key shared by two parties of communication in advance. Figure 5 gives a quantum circuit implementing rotation transformation for stego image with size $2^q \times 2^m \times 2^2$ based on the key $K_1 = k_3k_2k_1k_0$.

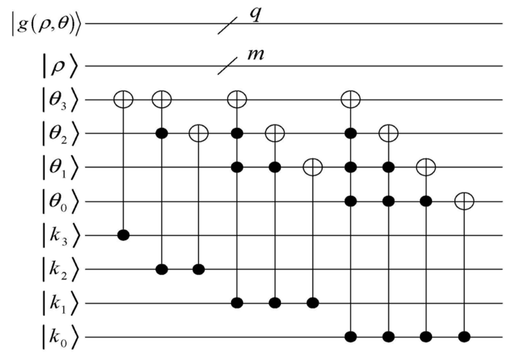

Figure 5. Quantum circuit implement of rotation transformation for stego image with size $2^q \times 2^m \times 2^2$ based on $K_1 = k_3k_2k_1k_0$

3.2 The Extracting Process

As a matter of facts, the process of extracting is the inverse process of embedding described in Section 3.1. Its main steps are presented as follows.

Step(1). According to the K_1, two parties of communication will share the third key K_2 to restore the original stego image.

Step(2). In this paper, it is clear that stego image is a complex vector in Hilbert space. So let decompose the vector Q of stego image into the direct product of gray scale and correspondingly position. The disintegrated vector Q is shown as the following Equation:

$$Q = a_0 \otimes \begin{pmatrix} 1 \\ 0 \\ 0 \\ \vdots \\ 0 \\ 0 \end{pmatrix}_{2^{m+n}} + a_1 \otimes \begin{pmatrix} 0 \\ 1 \\ 0 \\ \vdots \\ 0 \\ 0 \end{pmatrix}_{2^{m+n}} + \cdots + a_{2^{m+n}-2} \otimes \begin{pmatrix} 0 \\ 0 \\ 0 \\ \vdots \\ 1 \\ 0 \end{pmatrix}_{2^{m+n}} + a_{2^{m+n}-1} \otimes \begin{pmatrix} 0 \\ 0 \\ 0 \\ \vdots \\ 0 \\ 1 \end{pmatrix}_{2^{m+n}} \quad (27)$$

Obviously, this step can be realized because the vector Q and the binary sequence of position are known. After converting every first part (gray scale) of the direct product to binary sequence, it is necessary to read each binary sequence for knowing the LSQbs. In this example, it means converting a_0, a_1, ..., $a_{2^{m+n}-2}$ and $a_{2^{m+n}-1}$ to the appropriate binary sequence, i.e., a_{0_b}, a_{1_b}, ..., $a_{\left(2^{m+n}-2\right)_b}$ and $a_{\left(2^{m+n}-1\right)_b}$. The a_{i_b} stands for the gray's binary sequence of the i_{th} pixel in stego image.

Step(3). The last step is to extract the LSQb of every binary sequence. Based on the understanding of matrix coding, those LSQbs can restore the information about gray scale of quantum watermark image. According to the preparation of QUALPI in Ref [8], these qubits information can be restored to the original quantum watermark image, as a result.

Therefore, the utilization rate and the embedding rate of the new algorithm are 42.86% and 3.43, respectively.

4 The Simulation Result and Performance Analysis

In this section, some simulation results and performance analysis of the new algorithm are given. The size of four carrier gray images is 256×256, i.e., "Girl", "Lena", "Woman" and "Vegetables". And the size of four watermark binary images is 128×128, i.e., "Boy", "Map", "Ribbon" and "HTC". All experiments are simulated on the MATLAB R2012a.

4.1 Robustness

Robustness shows that quantum watermark image can be effectively extracted from stego image which was subjected to various attacks. In order to defend different geometric attacks, the new algorithm utilizes two important properties of log-polar sampling, i.e., rotation and scale invariances. These invariances make quantum watermark image extracted having a good robustness.

In order to prove the argument, Figure 6 is given to represent different geometric attacks, such as rotation, vertical axisymmetry, horizontal axisymmetry and scaling. The simulation results show that the new algorithm has good robustness.

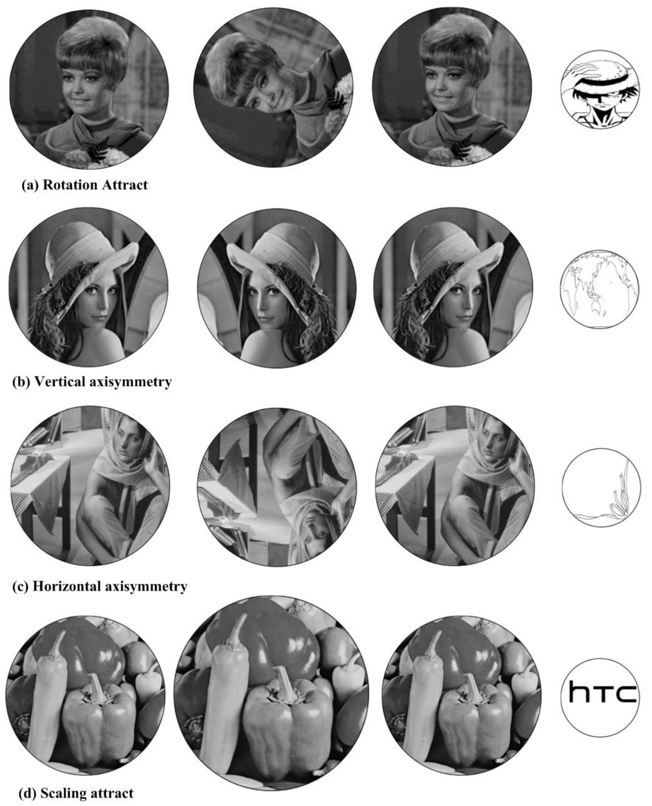

Figure 6. There are four groups of images. For each group, the left is carrier image, the second is attracted stego image by different geometric attacks, the third is restored into the original stego image, and the right is extracted watermark image

4.2 Transparency

Transparency reflects the similarity between carrier image and stego image. In Figure 6, it is easy to know that carrier images and the original stego images are incapable to be identified by the naked eye of human being.

At present, there is no specific evaluation standard for visual quality index of the quantum image. In this paper, the gray histogram and the classical peak signal to noise ratio (PSNR) are applied to evaluate transparency of the new algorithm.

The gray histogram is one of the simplest tools extensively used in digital image processing. It describes an image's gray content. An image histogram illustrates how pixels in an image are distributed by plotting the number of pixels at each gray level. Specifically, the gray histogram should not leak any information about watermark image or the relationship between carrier image and its stego image.

Here, gray histograms of carrier image and the corresponding stego image are shown in Figure 7 and Figure 8, respectively. It is clearly seen that the histogram of stego image is fairly uniform and significantly different from that of carrier image, so that it does not provide any clue to statistical attacks.

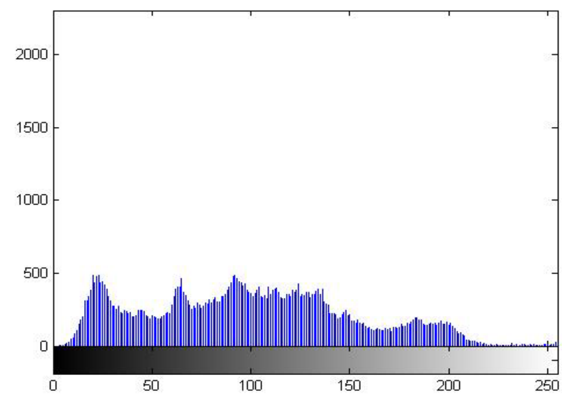

Figure 7. The gray histogram of carrier image "Lena"

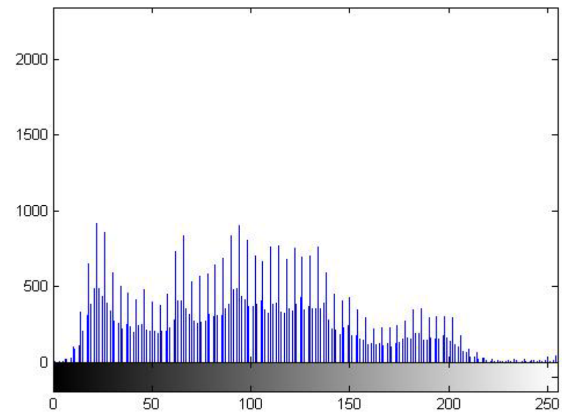

Figure 8. The gray histogram of stego image (carrier image is "Lena", and watermark image is "Map")

Let assume that there are two $2^m \times 2^n$ images *I* and *J* with the gray range 2^q, where *I* is the original carrier image and *J* is the corresponding stego image. $I(\rho,\theta)$ and $J(\rho,\theta)$ represent the gray values of the (ρ,θ) pixel. Mean squared error (MSE) and PSNR are defined as Equation (28) and (29), respectively:

$$MSE = \frac{1}{mn}\sum_{\rho=0}^{2^m-1}\sum_{\theta=0}^{2^n-1}\left[I(\rho,\theta)-J(\rho,\theta)\right]^2 \quad \textbf{(28)}$$

$$PSNR = 20\times\log_{10}\left(\frac{MAX_I}{\sqrt{MSE}}\right) \quad \textbf{(29)}$$

Here, MAX_I is the maximum possible pixel value of the image *I*.

Table 2 lists out the PSNR values of stego images obtained by embedding four different watermark images into four different carrier images, respectively. It can be found from Table 2 that the PSNR values of stego images are much higher than the image quality standard of 38*dB*, which proves that stego images have high image qualities.

Table 2. PSNR values (*dB*) of stego images in the simulation

	Boy	Map	Ribbon	HTC
Girl	55.8352	56.0182	56.0182	55.8266
Lena	56.3164	55.2795	56.1085	56.0724
Woman	55.2359	55.2763	55.7178	56.0952
Vegetables	55.7416	55.3241	55.8435	55.7924

In summary, the new algorithm has good performance in transparency.

4.3 Capacity

Capacity can be accurately calculated by the embedding rate. In this paper, based on matrix coding with *k*=3 and *n*=7 used in the new algorithm, it is easy to know that the embedding rate is 3.43. Furthermore, its utilization rate is 42.86%. As shown in Table 1, the larger *k* is, the lower the utilization rate of carrier data will be, which is equivalent to capacity of watermark. Comparing with the previous achievements, due to high embedding efficiency and low modification rate, the utilization rate of the new algorithm or called as the capacity is little lower as a sacrifice of improvements of robustness and transparency.

5 Conclusion

In this paper, a high efficient and robust quantum watermarking algorithm is proposed to better protect copyright of quantum images, which is based on QUALPI representation model, matrix coding and the LSQb modification technique. The new algorithm can obtain a good robustness to effectively resist on various geometric attacks, including rotation attack, flip attack and scaling attack. In terms of matrix coding and the LSQb modification technique, the new algorithm also can achieve great transparency for high embedding efficiency and low modification rate. For example, if *k*=3 and *n*=7, the utilization rate, the embedding efficiency and the modification rate of the new algorithm are 42.86%, 3.43 and 29.2%, respectively. Meanwhile, the larger the values of k and n are selected, the higher its embedding efficiency and the smaller its modification rate are. At final, the simulation results based on MATLAB show that the new algorithm has a good performance in robustness and transparency.

However, there still is a defect of low watermark capacity for the new algorithm as a sacrifice to improve robustness and transparency. As a compensation, besides of LSB, sub-LSB of pixels can be introduced to embed watermark image for doubling watermark capacity. Since the modification rate is low by adopting matrix coding, two least significant bits are modified simultaneously could have minor impacts to transparency of watermark as a result. In the future, our next research will be focused on the research of robust quantum watermarking algorithm to deal with more complex attacks, such as filtering and compression, which also can keep good balance between robustness and transparency.

Acknowledgements

This work was supported by the National Natural Science Foundation of China (No. 61373131, 61303039, 61232016, 61501247), the Six Talent Peaks Project of Jiangsu Province (Grant No. 2015-XXRJ-013), Natural Science Foundation of Jiangsu Province (Grant No. BK20171458), the Natural Science Foundation of the Higher Education Institutions of Jiangsu Province (China under Grant No.16KJB520030), Sichuan Youth Science and Technique Foundation (No.2017JQ0048), NUIST Research Foundation for Talented Scholars (2015r014), PAPD and CICAEET funds.

References

[1] X. Y. Chen, S. Chen, Y. L. Wu, Coverless Information Hiding Method based on the Chinese Character Encoding, *Journal of Internet Technology*, Vol. 18, No. 2, pp. 313-320, March, 2017.

[2] Z. H. Xia, X. Li, Coverless Information Hiding Method based on LSB of the Character's Unicode, *Journal of Internet Technology*, Vol. 18, No. 6, pp. 1353-1356, November, 2017.

[3] S. E. Venegas-Andraca, S. Bose, Storing, Processing and Retrieving an Image using Quantum Mechanics, *Quantum Information and Computation, Vol. 5105*, Orlando, Florida, 2003, pp. 1085-1090.

[4] S. E. Venegas-Andraca, J. L. Ball, Processing Images in Entangled Quantum Systems, *Quantum Information Processing*, Vol. 9, No. 1, pp. 1-11, February, 2010.

[5] J. I. Latorre, *Image Compression and Entanglement*, http://arxiv.org/abs/quant-ph/0510031

[6] P. Q. Le, F. Y. Dong, K. Hirota, A Flexible Representation of Quantum Images for Polynomial Preparation, Image Compression, and Processing Operations, *Quantum Information Processing*, Vol. 10, No. 1, pp. 63-84, February, 2011.

[7] Y. Zhang, K. Lu, Y. H. Gao, M. Wang, NEQR: A Novel Enhanced Quantum Representation of Digital Images, *Quantum Information Processing*, Vol. 12, No. 8, pp. 2833-2860, August, 2013.

[8] Y. Zhang, K. Lu, Y. H. Gao, K. Xu, A Novel Quantum Representation for Log-polar Images, *Quantum Information Processing*, Vol. 12, No. 9, pp. 3103-3126, September, 2013.

[9] J. Z. Sang, S. Wang, Q. Li, A Novel Quantum Representation for Color Digital Images, *Quantum Information Processing*, Vol. 16, No. 2, pp. 1-14, February, 2017.

[10] B. J. Chen, H. Z. Shu, G. Coatrieux, G. Chen, X. Sun, J. L. Coatrieux, Color Image Analysis by Quaternion-Type Moments, *Journal of Mathematical Imaging and Vision*, Vol. 51, No. 1, pp. 124-144, January, 2015.

[11] Z. H. Xia, X. H. Wang, L. G. Zhang, Z. Qin, X. M. Sun, K. Ren, A Privacy-preserving and Copy-deterrence Content-based Image Retrieval Scheme in Cloud Computing, *IEEE Transactions on Information Forensics and Security*, Vol. 11, No. 11, pp. 2594-2608, November, 2016.

[12] J. W. Wang, T. Li, Y. Q. Shi, S. G. Lian, J. Y. Ye, Forensics Feature Analysis in Quaternion Wavelet Domain for Distinguishing Photographic Images and Computer Graphics, *Multimedia Tools and Applications*, Vol. 76, No. 22, pp. 23721-23737, November, 2017.

[13] Y. P. Zhang, L. Chen, H. Hao, The New Audio Watermarking Algorithm Using Quantum Neural Networks, *Journal of Signal Processing*, Vol. 12, No. 9, pp. 3103-3126, June, 2013.

[14] L. Chen, B. Li, Y. P. Zhang, H. Hao, Improved Quantum Neural Networks based Audio Watermarking Algorithm, *Journal of PLA University of Science and Technology (Natural Science Edition)*, Vol. 14, No. 5, pp. 473-478, May, 2013.

[15] Q. Gao, R. H. Li, L. S. Liu, Blind Video Watermarking Algorithm Based on Correlations between Neighboring Frames, *Journal on Communications*, Vol. 27, No. 6, pp. 43-48, June, 2006.

[16] A. M. Iliyasu, Towards Realisation of Secure and Efficient Image and Video Processing Applications on Quantum Computers, *Entropy*, Vol. 15, No. 8, pp. 2874-2974, August, 2013.

[17] J. Z. Sang, S. Wang, Q. Li, Least Significant Qubit Algorithm for Quantum Images, *Quantum Information Processing*, Vol. 15, No. 11, pp. 4441-4460, November, 2016.

[18] X. H. Song, S. Wang, A. A. El-Latif, X. M. Niu, Dynamic Watermarking Scheme for Quantum Images based on Hadamard Transform, *Multimedia Systems*, Vol. 20, No.4, pp. 379-388, July, 2014.

[19] Y. G. Yang, X. Jia, P. Xu, J. Tian, Analysis and Improvement of the Watermark Strategy for Quantum Images Based on Quantum Fourier Transform, *Quantum Information Processing*, Vol. 12, No. 8, pp. 2765-2769, August, 2013.

[20] X. H. Song, S. Wang, S. Liu, A. A. El-Latif, X. M. Niu, A Dynamic Watermarking Scheme for Quantum Images using

Quantum Wavelet Transform, *Quantum Information Processing*, Vol. 12, No. 12, pp. 3689-3706, December, 2013.
[21] N. Jiang, N. Zhao, L. Wang, LSB Based Quantum Image Steganography Algorithm, *International Journal of Theoretical Physics*, Vol. 55, No. 1, pp. 107-123, January, 2016.
[22] S. Miyake, K. Nakamae, A Quantum Watermarking Scheme using Simple and Small-scale Quantum Circuits, *Quantum Information Processing*, Vol. 15, No. 5, pp. 1849-1864, May, 2016.
[23] A. Westfeld, F5-A Steganography Algorithm: High Capacity Despite Better Steganalysis, *4th International Workshop on Information Hiding*, Pittsburgh, PA, 2001, pp. 289-302.
[24] D. Wang, Z. H. Liu, W. N. Zhu, S. Z. Li, Design of Quantum Comparator Based on Extended General Toffoli Gates with Multiple Targets, *Computer Science*, Vol. 39, No. 9, pp. 302-306, September, 2012.

Biographies

Zhiguo Qu received the Ph.D. degree in information security from Beijing University of Posts and Telecommunications in 2011. Currently, he is a Lecturer in the School of Computer and Software, Nanjing University of Information Science and Technology in China. His research interests include quantum secure communication and quantum information hiding.

Zhenwen Cheng is a master candidate in electronics and communication engineering of Nanjing University of Information Science and Technology, China, in 2016. His research interests include quantum watermarking and quantum steganography.

Mingming Wang received the Ph.D. degree from the School of Computer Science, Beijing University of Posts and Telecommunications, China in 2013. Currently, he is a Lecturer in School of Computer Science, Xi'an Polytechnic University. His research interests include information security, quantum cryptography, etc.

Wenjie Liu received his Bachelor (HZAU, China, 1997), Master (WHU, China, 2004), Ph.D. (SEU, 2011). Currently, he is an associate professor of Computer Science at Nanjing University of Information Science and Technology, China. His research interests include quantum machine learning, quantum secure multi-party computation, quantum cryptography communication, etc.